Comprehensive Assessment of Laser Tube Bending Process by Response Surface Methodology

Mehdi Safari, Ricardo Alves de Sousa, and Jalal Joudaki*

M.S. and J. J.
Department of Mechanical Engineering, Arak University of Technology, Arak, 38181-41167, Iran.
E-mail: m.safari@arakut.ac.ir (ms_safari2005@yahoo.com)
R. A. D. S.
Center for Mechanical Technology and Automation, Department of Mechanical Engineering, University of Aveiro, Campus de Santiago, Aveiro, 3810-183, Portugal.

Keywords: laser tube bending process, main bending angle, lateral bending angle, interaction of parameters, response surface methodology

Abstract: The laser beam can be used as a powerful tool for bending tubes and sheets by local heating and buckling mechanism. In this paper, the bending of mild steel tubes will be investigated by irradiation of the laser beam. To consider the effect of the interaction of process parameters despite previous research, six laser tube bending process parameters in different levels including laser power, scanning speed, laser beam diameter, irradiation length, number of irradiation passes, and irradiation scheme are selected and set of 92 experimental tests planned according to the response surface methodology (RSM). The tests have been carried out by using a continuous wave (CW) CO2 laser. The influencing parameters affecting the main bending angle and lateral bending angle are determined. The effect of main process parameters and their interaction on the main and lateral bending angle are discussed either. The AIS creates a higher main bending angle compared to the CIS. The results show that the main bending angle and lateral bending angle increase by increasing the laser power, irradiation length, and the number of irradiation passes and reducing the scanning speed and laser beam diameter. The main and lateral bending angles are determined by a regression equation with about 96% goodness of fitting. The results show that 1100 W laser power, 14.6 mm/s scanning speed, 4 mm laser beam diameter, 28.27 mm irradiation length, 1 pass of irradiation, and axial irradiation scheme (AIS) lead to a simultaneous maximum bending angle of 1.80° and minimum lateral bending angle of 0.152°.

1. Introduction

The tube bending process is used widely in different industries such as automotive, shipbuilding, heat exchangers, hydraulic systems, boilers, and aircraft manufacturing industries. Mechanical bending processes such as the rotary draw bending process, compression bending process, and roll bending process bend the tubes by applying a mechanical force. Despite the simplicity of these processes, the changes in the dimensions of the bent tube can affect the operational performance of the tube. Precise bending angles, especially in high-strength tubes or low-diameter tubes were obtained by using the laser tube bending process (LTBP). Besides, the combination of mechanical bending processes and laser softening can enhance the maximum bending angle as well as decrease the deformation of the cross-section[1]. Springback is another important phenomenon in tube bending. The bending angle changes after the unloading of external force. However, this phenomenon was not observed in the LTBP and the tube bends during the cooling of the tube. Therefore, laser bending and laser forming are noncontact spring-back-free forming processes. Several pieces of research discuss the reasons for tube bending due to heating by the laser beam. The thermal stresses generated during the scanning of the tube by laser beam induce plastic deformation in specified zones and lead to bending of the tube. The main process parameters are usually laser power, beam diameter, scanning velocity, and the number of scans. The thermal stresses generated during laser scanning are strongly dependent upon laser beam geometry. These beam geometries sometimes lead to undesirable effects such as buckling and distortion in tube bending. The results show that tube bending by circular beam provides a slightly higher bending angle while much higher distortions will be obtained compared to other beam geometries[2, 3]. In addition, the appearance of many bending defects like wall thinning, wrinkling, and ovalization can be decreased and a more uniform part can be fabricated.

Li and Yao[4-6] are two researchers who have an important role in developing laser tube bending. A numerical model was developed to investigate the effect of strain rate on forming efficiency and stress distribution. In addition, the mechanisms of the process are explained to better understand the deformation characteristics such as wall thickness variation, cross-section ovalization, bending radius, and asymmetry. After validation of experimental results and FEM results, a closed-form equation had been proposed for the calculation of the bending angle in LTBP.

Zhang et al.[7] investigated four different scanning strategies for tube bending, including point-source circumferential scanning, pulsed line-source axial scanning strategy, and line-source axial scanning without and with water cooling. The four different scanning strategies

are investigated by a coupled thermomechanical finite element model. A pulsed line-source axial scanning strategy can deform the tube according to the beam coverage. Water cooling increases the bending deformation. The ovality and wall thickness variation is larger in axial scanning strategy (AIS) than that in circumferential scanning strategy (CIS). Also, the results show that the line-source axial scanning is better than the point-source circumferential scanning strategy.

Different tools and scanning strategies are utilized for finding the bending angle in LTBP. Khandandel et al.[8] proposed a new circular scanning strategy for the fabrication of 2D and 3D shapes. This strategy is presented in the form of two step-by-step and reverse schemes. Hsieh and lin[9] studied the laser bending of a thin 304 stainless steel tube by numerical simulation and experimental measurement. The Gaussian model was selected for modeling the laser beam and the 3D uncoupled thermal-mechanical elastic-plastic analysis was carried out to study the buckling phenomenon on the tube. It was shown that the buckling mechanism of thin metal tubes under laser forming was initiated by a uniform temperature distribution combined with plastic deformation.

Yadav et al.[10] utilized numerical simulations for investigation of the effect of line energy on the bending mechanisms of duplex stainless steel. In addition, the effect of temperature distribution at the bottom surface on the bend angle has been studied. The results show that at constant line energy, the bend angle increases with the increase in laser power and scanning speed.

Imhan et al.[11] focused on experimental, analytical modeling, and numerical simulation to give more understanding of the process. An analytical model has been used to determine the bending angle by using MATLAB software. The changes in material specification during the LTBP due to the temperature rise have been studied. Particle Swarm Optimization (PSO) was used to optimize the analytical and experimental results and reduce the mean absolute error. Keshtiara et al.[12] studied the effects of laser beam process parameters (laser power, laser beam diameter, scanning speed, and circumferential scanning angle) on the bending angle, ovality, thickening, and energy consumption. The design of experiments has been carried out by the L27 Taguchi method. Finite element analysis and artificial neural networks (ANN) were used for data analysis and multi-objective optimization concerning the laser forming parameters were carried out using a genetic algorithm (GA). The objectives include maximum bending angle, minimum ovality, minimum thickening, and minimum energy consumption. The results showed that the laser beam power, the laser beam coverage, and the laser beam speed are the most influential parameters of tube bending. By combining the abilities of GA

and ANN, it is possible to bend a tube with a specific bending angle and curvature radius with the least ovality, the least thickening, and the least forming energy consumption. As can be seen, several tools such as ANN, GA, and PSO … can be used for process optimization. In addition, statistical modeling using the design of experiments methods such as full-factorial and response surface methodology (RSM) was used in similar research[13-15] to discover a regression model for complicated system identification.

The authors published several articles about laser bending[16-21]. The authors studied the effect of irradiation scheme, laser power, and irradiation length of laser beam[20] in LTBP. The authors believe that the main shortcoming in LTBP is the complexity of geometry and lack of comprehensive investigations in different irradiation conditions. Most of the researchers focused on sheet bending and different aspect of LTBP was not investigated comprehensively. Also, the material of the investigation can affect the results. As can be seen, stainless steel 304[9, 12] and duplex stainless steel[10] are two common materials investigated due to their application in industries. Mild steel is another material that has low cost and is widely used in industries[16-18, 20-22].

The literature survey shows that the bending of tubes is very complicated and researchers tried to find different aspects of LTBP. Most of the research focuses on the effect of main process parameters while interactions of the process parameters are important and they were neglected for decreasing the number of required experiments and decreasing the cost of experiments. In this paper, a comprehensive study will be implemented to find the effect of process parameters and their interaction on the bending angle of tubes. Six process parameters including laser power, scanning speed, laser beam diameter, irradiation length, number of irradiations, and the irradiation scheme are selected as the influencing process parameters. A design of experiments will be carried out and the main bending angle and lateral bending angle will be measured and analyzed for a set of 92 experiments designed by RSM. The main novelty of the current work is considering and analyzing the effect of all selected process parameters simultaneously to find all aspects of bending angle by laser beam irradiation which was not implemented previously. In many previous studies, only the effect of the main process parameters considered in the investigation and the interaction of the process parameters were ignored to reduce the number of experiments. The goal of the current study is to inspect the interaction of the mentioned process parameters interactions and find the best and proper conditions in the range of study for maximizing the main bending angle and minimizing the lateral bending angle.

2. Experimental Work

The materials and laser machine used in this study are similar to the recently published article by the authors[20]. An AMADA CO_2 laser was used for laser tube bending. The laser machine produces a continuous wave (CW) laser beam. The intensity distribution of the laser beam was Gaussian distribution (default of machine setup). The material used in this study is mild steel tubes with 100 mm length, 18 mm outer diameter, and 1mm thickness. The chemical composition of the tube is reported in Table 1. The outer surface of the tube has been covered by graphite powder to enhance the laser beam absorption. The graphite powder was sprayed on the surface of the specimens to create a uniform thickness layer. The thickness of the layer was measured by a thickness-meter device and it was controlled that the thickness of the sprayed layer was thicker than 1 mm. The tube is clamped from one side by a 3-jaw lathe chuck. Six important process parameters were selected as influencing parameters which include laser power, scanning speed, laser beam diameter, irradiation length, number of irradiations, and irradiation scheme. Three of them (laser power, scanning speed, and laser beam diameter) were adjusted in the laser machine, and the others were independent of the laser machine. The authors carried out some experiments and find the proper range of laser tube bending. The main challenge in the selection of process parameters is excessive heating of the tube which leads to melting or creating a hole in the tube. Three levels were selected for laser tube bending and only the irradiation scheme has two levels (Circular Irradiating Scheme (CIS), Axial Irradiating Scheme (AIS)). Table 2 shows the levels of process parameters in which the current study has been conducted. The irradiation length (arc) reported in Table 2 was the angle of the scanning path in the CIS scheme (20, 100, and 180°) and the equivalent length of the irradiated arc (respectively 3.14, 15.70, and 28.27 mm) was the irradiation length in AIS. The laser beam irradiated along the centerline of the tube is symmetrical from the midplane of the tube in AIS. Also, the laser beam irradiated symmetrically at the midplane of the tube in CIS. Figure 1(a) shows the AIS and CIS irradiation schemes. The heat intensity in the laser beam is very high and a narrow region experiences an increase in temperature. Meanwhile, the temperature decrease after irradiation is fast and between repetitive passes, enough time is left for cooling the tube up to room temperature (5 minutes). Figure 1(a) shows the schematic view of multi-pass LTBP in AIS and CIS irradiation patterns. In CIS irradiation, each pass of the laser beam irradiation starts from the finish point of the previous irradiated pass (after cooling the tube). Response surface

methodology (RSM) was used for the design of experiments. The RSM helps the researcher to find the effect of process parameters and their interaction with less number of experiments compared to a full-factorial design. A total of 92 experiments (according to Box-Behnken design) have been carried out and the list of them is available in Table A.1 Appendix. Because of the large number of experiments, there is not possible to repeat all of the experiments. Nevertheless, randomly three specimens were prepared for ten experiments, and the bending angle was measured. The results show that the laser bending experiments were repeatable. After reaching the temperature of the tube to room temperature, the main bending angle and lateral bending angle were measured by a coordinate measuring machine (CMM). Fig. 1(b) shows the main and lateral bending angles for a laser-bent tube schematically. The lateral bending angle is undesired and decreases the geometrical tolerance of the bent tube. It happens due to non-homogeneous heating at the start and end of the irradiation path. The main bending angle and lateral bending angle were measured by an Easson ENC-565 coordinate measuring machine. The main bending angle and lateral bending angle are defined in two planes perpendicular to the cross-section of the tube as shown in Figure 1(b). The point cloud of CMM data was analyzed and the main bending angle and lateral bending angle were determined. According to the used laser beam diameters and the wall thickness of the tube, in the present research, the buckling mechanism will be activated leading to the bending of the tubes.

Table 1. Chemical composition of mild steel

Element	Fe	C	Cu	Mn	P	S	Si
Content (%)	98.0	0.23	0.20	0.83	0.04	0.05	0.28

Table 2. The range of process parameters variation in experimental tests

Process Parameters	Abbreviation	value
Laser Power (W)	P	500 800 1100
Scanning Speed (mm/s)	S	10 15 20
Laser Beam Diameter (mm)	D	4 6 8
Irradiation length (arc) in CIS (degree)	L	20 100 180
Number of Irradiation Passes	N	1 3 5
Irradiation Scheme	Sch.	Circular Irradiating Scheme (CIS) Axial Irradiating Scheme (AIS)

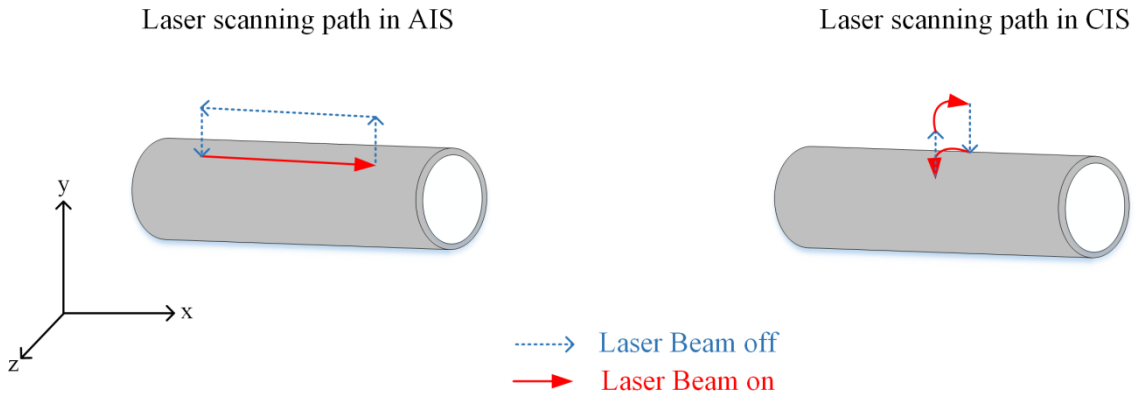

(a)

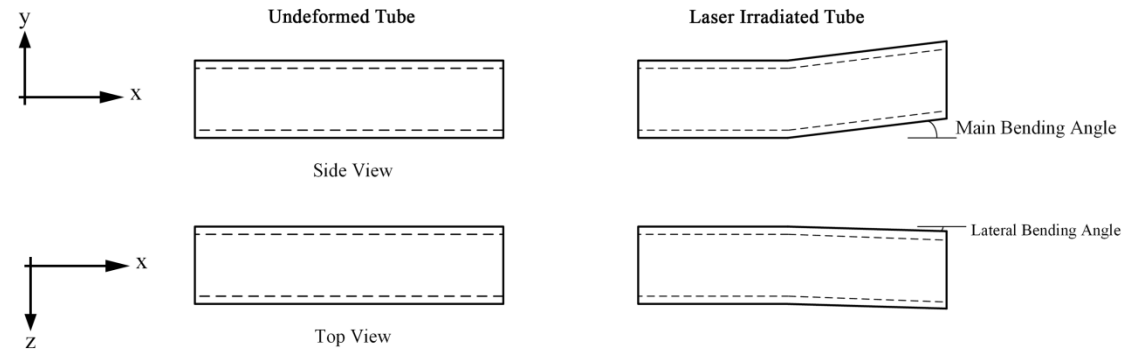

(b)

Figure 1. a) AIS and CIS irradiation scheme in multi-pass LTBP, b) Schematic views of main and lateral bending angles

3. Results and Discussion

3.1. Effect of process parameters on Main Bending Angle

After measuring the main bending angle, the results were analyzed by statistical tools prepared by Minitab software. Table 3 the results of the Analysis of Variance (ANOVA). The last column (P-Value) is important and if the value was greater than 0.05, it means that this parameter has little effect on the output. The results show that all selected process parameters are significant and should be included in the investigation. The greater F-Value shows the higher impact of the process parameters and the Pareto chart was plotted according to the results as Figure 2. The most influencing process parameter is the irradiation schemes and after that the laser power and irradiation length are important. The main bending angle can be calculated by Equations 1 and 2 for the range of process parameters shown in Table 2. The coefficient of determination (R2) is 96.49% which shows the goodness of fitting. It is worth noting that the interaction of laser power and the number of irradiation passes is the only

interaction in influential process parameters and other interactions are negligible according to statistical analysis.

Sch	Equation	
AIS	$Main\ Bending\ angle = 1.2846 + 0.000818\,P - 0.028870\,S + 0.02360\,D + 0.000260\,L - 0.02357\,N - 0.000001\,P^2 + 0.000467\,S^2 - 0.003238\,D^2 + 0.000005\,L^2 + 0.008475\,N^2 + 0.000004\,P \times N$	(1)
CIS	$Main\ Bending\ angle = 1.0852 + 0.000818\,P - 0.028870\,S + 0.02360\,D + 0.000260\,L - 0.02357\,N - 0.000001\,P^2 + 0.000467\,S^2 - 0.003238\,D^2 + 0.000005\,L^2 + 0.008475\,N^2 + 0.000004\,P \times N$	(2)

Table 3. The analysis of variance in experimental tests for main bending angle

Source	DF	Adj SS	Adj MS	F-Value	P-Value
Model	12	2.16007	0.180006	36398.78	0.000
Linear	6	2.09838	0.349730	70718.37	0.000
P	1	0.57459	0.574592	116187.53	0.000
S	1	0.17645	0.176446	35678.97	0.000
D	1	0.02979	0.029788	6023.30	0.000
L	1	0.28525	0.285248	57679.74	0.000
N	1	0.11737	0.117370	23733.27	0.000
Sch	1	0.91493	0.914933	185007.45	0.000
Square	5	0.06165	0.012331	2493.39	0.000
P*P	1	0.00808	0.008082	1634.26	0.000
S*S	1	0.00238	0.002382	481.68	0.000
D*D	1	0.00293	0.002929	592.19	0.000
L*L	1	0.01513	0.015134	3060.18	0.000
N*N	1	0.02006	0.020057	4055.72	0.000
2-Way Interaction	1	0.00004	0.000040	8.19	0.005
P*N	1	0.00004	0.000040	8.19	0.005
Error	79	0.00039	0.000005		
Lack-of-Fit	69	0.00039	0.000006	*	*
Pure Error	10	0.00000	0.000000		
Total	91	2.16046			

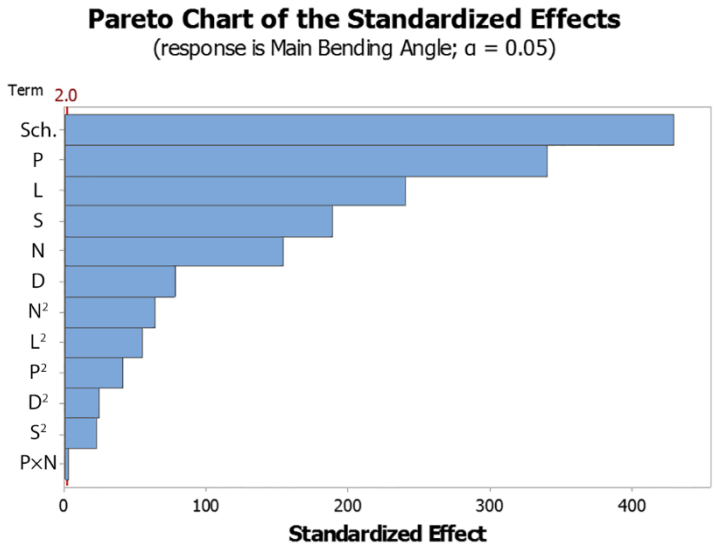

Figure 2. The Pareto chart for the main bending angle

Figure 3(a) shows the effect of selected process parameters on the mean of the main bending angle. The results show that increasing laser power, length of irradiation, and the number of irradiation passes cause increasing the bending angle while increasing scanning speed and laser beam diameter cause a decrease in the main bending angle. The effect of the irradiation scheme is also important and similar to previous research, the axial irradiating scheme (AIS) can create higher main bending angles compared to the circular irradiating scheme (CIS). Figure 3(b) shows the interaction of all process parameters. The results show that the effect of irradiation scheme and laser power are the most influential process parameters and laser beam diameter is the weakest parameter that affects the main bending angle.

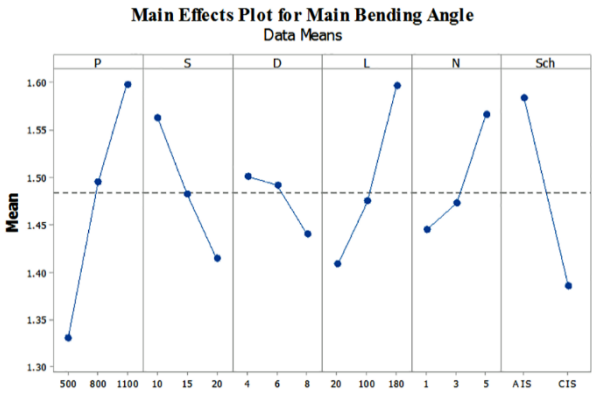

(a)

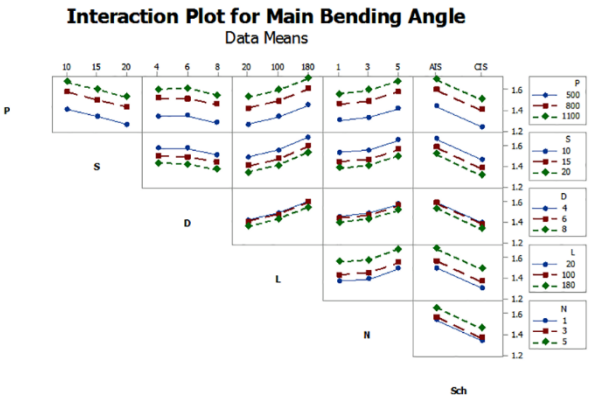

(b)

Figure 3. Effect of process parameters on a) the mean of the main bending angle, b) interaction on the main bending angle

Figure 4(a) shows the 3D response surface for the interaction of laser power and the number of irradiation passes and Figure 4(b) shows a 2D contour plot of the parameters. As mentioned previously, only the interaction of laser power and the number of irradiation passes is influential and other interactions are negligible. The interaction of laser power and number of irradiation is positive and by increasing the laser power and number of irradiation, the main bending angle increases slightly. This relates to the amount of heat transferred in repetitive passes of laser beam irradiation.

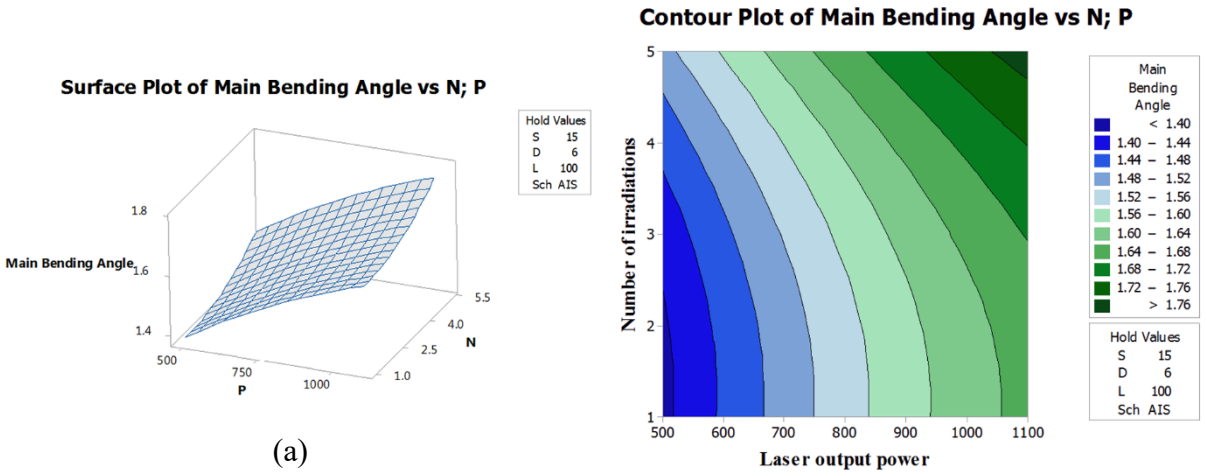

Figure 4. Variation of the main bending angle by the laser power and the number of irradiation passes a) 3D surface plot, b) contour plot

Previous research[20] shows that the AIS scheme of laser beam irradiation leads to a higher bending angle compared to the CIS scheme. It is because of inducing plastic strains in several sections along the length of the tube in the AIS scheme compared to inducing the plastic strain in just one cross-section through the tube length in the CIS scheme. A higher plastic deformation zone in the irradiated tube and the stiffness of the tube leads to increasing the bending angle. By increasing the laser power and the number of irradiation passes, the amount of heat flux transferred to the tube increases and higher plastic deformations in the irradiated zones will be induced and consequently the main bending angle increases[16]. By increasing the irradiation length in the AIS scheme, the main bending angle increases because the main

bending angle relates to the sum of plastic strains created in different cross-sections[16], and increasing the irradiation length involves more sections in laser tube bending. In addition, increasing the irradiating length, thickening in intrados, and thinning in extrados of the tube help to obtain a higher main bending angle[21].

3.2. Effect of process parameters on Lateral Bending Angle

Table 4 the results of the Analysis of Variance (ANOVA) prepared statistical analysis tool of Minitab software. The results show that all selected process parameters are significant and the order of importance is different from the main bending angle assessment. Figure 5 shows the Pareto chart which was plotted according to the effectiveness of process parameters. The most influential process parameter is the irradiation schemes and after that the number of irradiation, scanning speed, and laser power are important. The lateral bending angle can be calculated by Equations 3 and 4 for the range of process parameters shown in Table 2. The coefficient of determination (R2) is 95.98% which shows the goodness of fitting. The results show that the square of process parameters except for the length of irradiation (and also irradiation scheme which is a qualitative parameter) is important and affect the lateral bending angle. Six interactions (of ten existing interactions) are important which are P×S, P×D, P×L, S×D, S×L, and D×L. All interactions related to the number of irradiation are ineffective.

Sch	Equation	
AIS	$$\begin{aligned} \textit{Lateral Bending angle} = {} & 0.18257 + 0.000028\,P - 0.006495\,S + 0.00151\,D \\ & - 0.000212\,L + 0.017777\,N - 0.000001\,P^2 + 0.000050\,S^2 - 0.000956\,D^2 \\ & - 0.001713\,N^2 + 0.000002\,P \times S + 0.000004\,P \times D + 0.000000\,P \times L \\ & + 0.000250\,S \times D + 0.000006\,S \times L + 0.000013\,D \times L \end{aligned}$$	(3)
CIS	$$\begin{aligned} \textit{Lateral Bending angle} = {} & 0.20263 + 0.000028\,P - 0.006495\,S + 0.00151\,D \\ & - 0.000212\,L + 0.017777\,N - 0.000001\,P^2 + 0.000050\,S^2 - 0.000956\,D^2 \\ & - 0.001713\,N^2 + 0.000002\,P \times S + 0.000004\,P \times D + 0.000000\,P \times L \\ & + 0.000250\,S \times D + 0.000006\,S \times L + 0.000013\,D \times L \end{aligned}$$	(4)

Table 4. the analysis of variance in experimental tests for main bending angle

Source	DF	Adj SS	Adj MS	F-Value	P-Value
Model	16	0.022124	0.001383	714.76	0.000
Linear	6	0.020553	0.003425	1770.68	0.000
P	1	0.001512	0.001512	781.84	0.000
S	1	0.002076	0.002076	1072.93	0.000
D	1	0.000338	0.000338	174.62	0.000

L	1	0.000176	0.000176	90.79	0.000
N	1	0.007200	0.007200	3721.83	0.000
Sch	1	0.009251	0.009251	4782.07	0.000
Square	4	0.001300	0.000325	167.97	0.000
P*P	1	0.000252	0.000252	130.36	0.000
S*S	1	0.000029	0.000029	15.18	0.000
D*D	1	0.000276	0.000276	142.42	0.000
N*N	1	0.000885	0.000885	457.54	0.000
2-Way Interaction	6	0.000271	0.000045	23.38	0.000
P*S	1	0.000050	0.000050	25.85	0.000
P*D	1	0.000050	0.000050	25.85	0.000
P*L	1	0.000050	0.000050	25.85	0.000
S*D	1	0.000050	0.000050	25.85	0.000
S*L	1	0.000039	0.000039	20.29	0.000
D*L	1	0.000032	0.000032	16.60	0.000
Error	75	0.000145	0.000002		
Lack-of-Fit	65	0.000145	0.000002	*	*
Pure Error	10	0.000000	0.000000		
Total	91	0.022269			

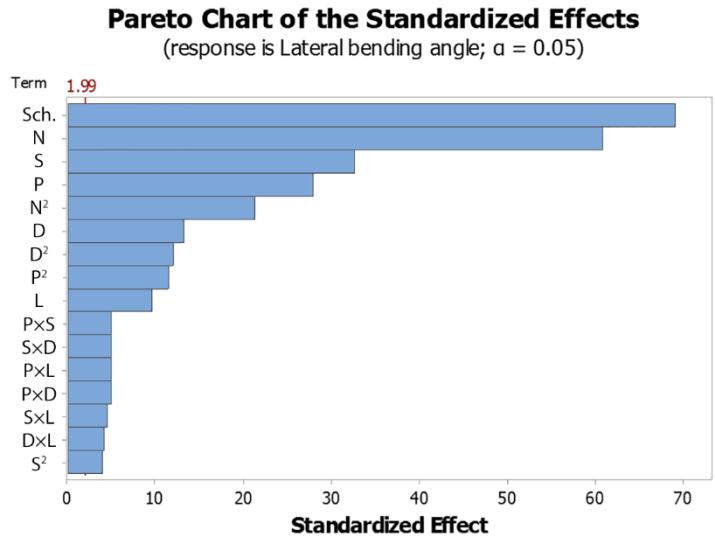

Figure 5. The Pareto chart for the main bending angle

Figure 6(a) shows the effect of selected process parameters on the mean of lateral bending angle. The trends of variation are similar between the main bending angle and lateral bending angle. The lateral bending angle increases by increasing the laser power, length of irradiation, and the number of irradiation passes and reduces by increasing the scanning speed and laser beam diameter. So, the process parameters increase the main bending angle, increase the

lateral bending angle. The effect of the irradiation scheme differs between the main bending angle and lateral bending angle. The circular irradiating scheme (CIS) creates a higher lateral bending angle. Figure 6(b) shows the interaction of all process parameters. The results show that the effect of the number of irradiation is the most influential process parameter and the irradiation length and the laser beam diameter are the weakest parameters that affect the lateral bending angle.

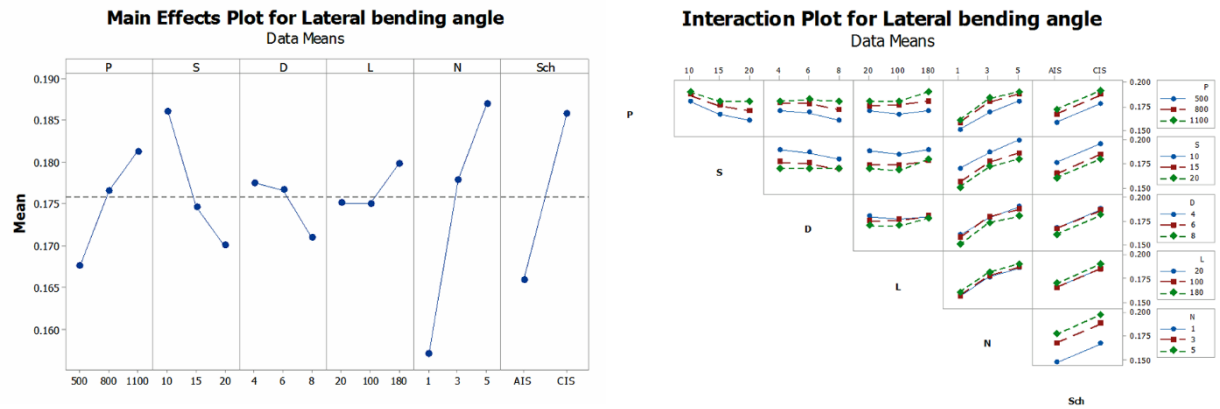

(a) (b)

Figure 6. Effect of process parameters on the a) means of the main bending angle, b) interaction of the main bending angle

Figure 7(a) shows the contour plot for the interaction of laser power and scanning speed. The lateral bending angle increases by increasing the laser power and decreasing the scanning speed. For minimizing lateral bending angle which is an unwanted phenomenon, lower laser power, and higher scanning speed should be utilized. Figure 7(b) shows the contour plot of laser power and laser beam diameter. At low laser power, increasing beam diameter cause decreasing the lateral bending angle while at higher laser power, the maximum laser beam diameter obtained at 6 mm and lower or higher values from this value causes decreasing the lateral bending angle. Figure 7(c) shows the contour plot of laser power and irradiation length. At low laser power, the effect of irradiation length on the lateral bending angle is almost negligible while at higher laser power, increasing the irradiation length causes increasing lateral bending angle. So, for minimizing the lateral bending angle, low laser power, high scanning speed, and high laser beam diameter should be utilized.

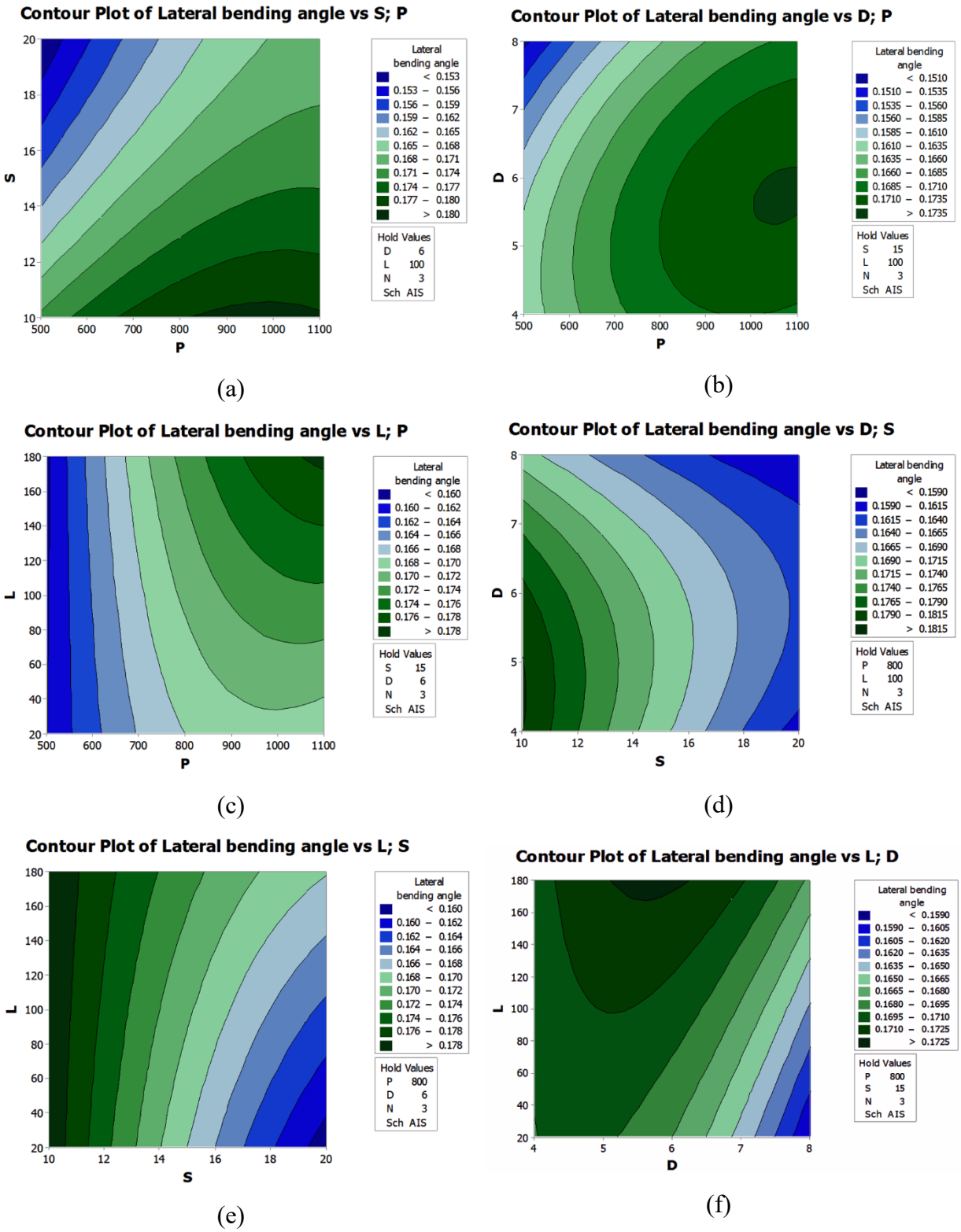

Figure 7. Contour plot of the variation of the lateral bending angle by a) the laser power and scanning speed b) the laser power and laser beam diameter c) the laser power and irradiation length d) the scanning speed and laser beam diameter e) the scanning speed and irradiation length f) the laser beam diameter and irradiation length

Figure 7(d) shows the contour plot of scanning speed and laser beam diameter. Similar to Figure 7(b), the variation of lateral bending angle about 6 mm laser beam diameter has extremum. Figure 7(e) shows the contour plot of scanning speed and irradiation length. At low scanning speed, the effect of irradiation length is negligible but at a higher value of scanning speed, more irradiation length causes more lateral bending angle. Also, by increasing the scanning speed, the lateral bending angle decreases.

Figure 7(f) shows the contour plot of laser beam diameter and irradiation length. Interaction of irradiation length and laser beam diameter is important. Interaction of laser beam diameter with scanning speed and laser power shows that about 6mm beam diameter is almost symmetric. But the interaction of irradiation length and laser beam diameter is not symmetric and a higher beam diameter leads to a lower lateral bending angle. At lower laser beam diameter, the effect of laser irradiation length becomes negligible but at higher laser beam diameter, low irradiation length cause reduced lateral bending angle.

The main bending angle increases by increasing laser irradiation length and decreasing laser beam diameter, while the lateral bending angle decreases by increasing laser beam diameter and decreasing irradiation length. Figure 8 shows all levels of the interaction of process parameters. The main bending angle is obtained by higher laser power, low scanning speed, low laser beam diameter, and higher irradiation length. For all mentioned conditions except irradiation length, lateral bending angle increases. The main bending angle is obtained by low scanning speed, low laser beam diameter, and higher irradiation length, and these conditions lead to maximum lateral bending angle. Comparison of Figure 3(a) and Figure 6(a) show similar trends for all process parameters except the irradiation scheme. Higher main bending angle and lower lateral bending angle obtained by axial irradiation scheme (AIS). Increasing the number of irradiation passes, increases the main bending angle but it has more effect on the lateral bending angle than the main bending angle.

When the surface is irradiated by the laser beam, surface expansions occur and then the surface contractions occur when the laser beam passes through it. The amount of created contraction is not necessarily equivalent to the amount of expansion, and this creates a slight lateral bending angle in the tube. As the irradiation process continues in the next passes of irradiation, it causes expansion and contraction again, as well as due to the bending stiffness in the tube due to the irradiation of the previous stage, the amount of lateral bending angle increases. For this reason, despite irradiating the tube with the axial path, a slight lateral bending angle is created. This issue is also mentioned in Safdar et al.[3].

At last, it should be noted that the lateral bending angle is an unwanted and undesired effect and asymmetry in laser beam irradiation cause its creation of it. Complicated scanning strategies such as spiral irradiation can increase it, but in this study, only the AIS and CIS were investigated. It can be a good opinion for future works to design scanning strategies to minimize this asymmetry and lateral bending angle.

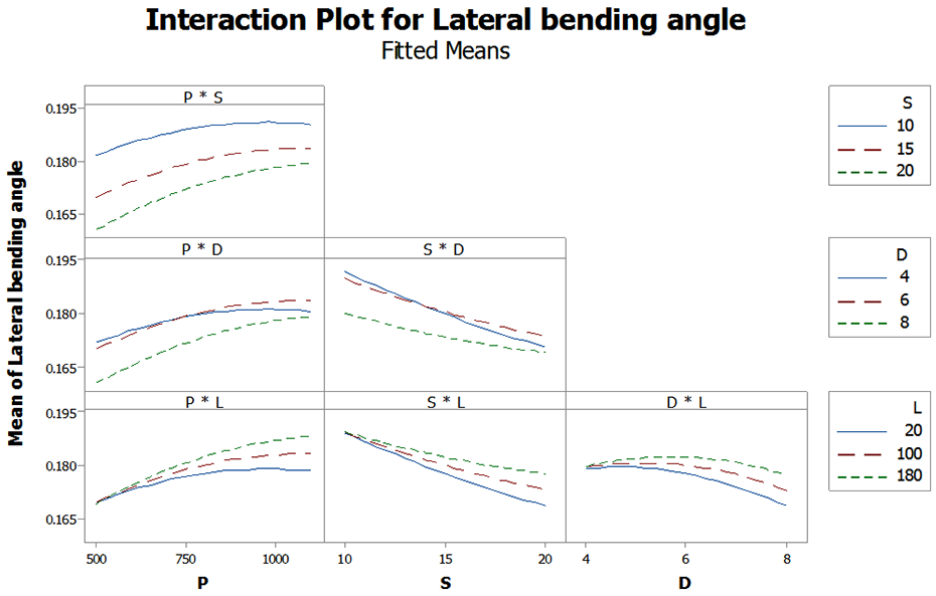

Figure 8. effect of process parameters interaction on the lateral bending angle

3.3. Optimal Condition

Figure 9 shows the optimal condition of process parameters for maximized bending angle, minimum lateral bending angle and concurrent maximized bending angle, and minimum lateral bending angle. Maximized bending angle obtained at 1100 W laser power, 10 mm/s scanning speed, 4 mm laser beam diameter, 28.27 mm irradiation length, 5 passes of irradiation, and axial irradiation scheme (AIS) and leads to 2.00° main bending angle. In mentioned condition, the lateral bending angle will be 0.1885°. Minimum lateral bending angle obtained at 500 W laser power, 20 mm/s scanning speed, 8 mm laser beam diameter, 3.14 mm irradiation length, 1 pass of irradiation, and axial irradiation scheme (AIS) and leads to 0.1175° lateral bending angle and 1.174° main bending angle. For simultaneous maximum bending angle and minimum lateral bending angle, process parameters should be set as 1100 W laser power, 14.6 mm/s scanning speed, 4 mm laser beam diameter, 28.27 mm irradiation length, 1 pass of irradiation, and axial irradiation scheme (AIS) and leads to 1.80° main bending angle and 0.152° lateral bending angle. The proper condition for maximum main bending angle and minimum lateral bending angle is determined and the main and lateral

bending angle can be calculated by the obtained regression equations with very good fitting quality.

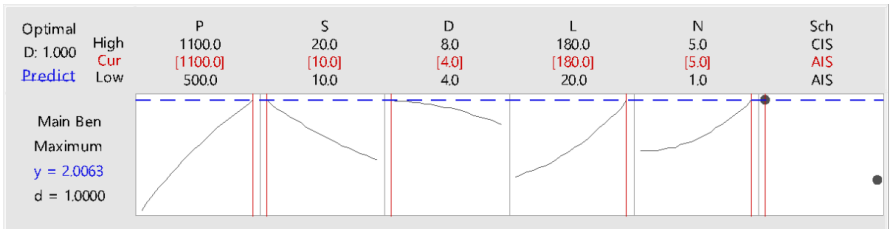

(a)

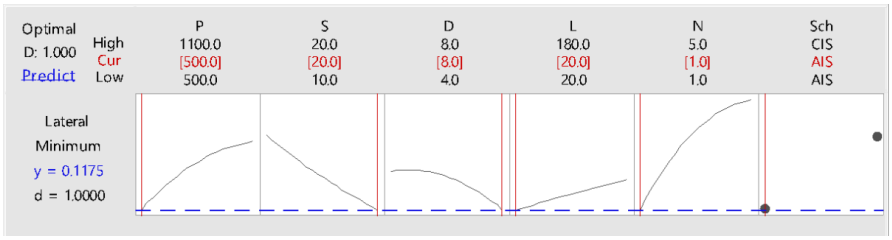

(b)

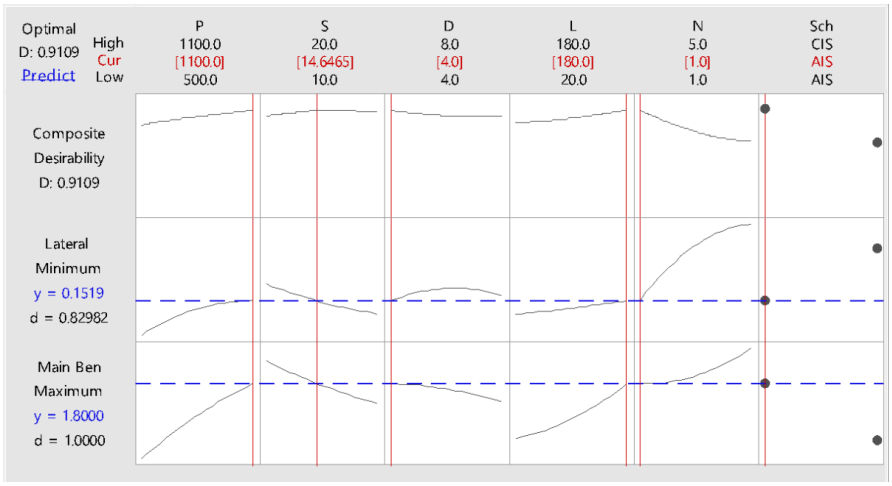

(c)

Figure 9. The optimal condition for a) maximized main bending angle b) minimized lateral bending angle, c) simultaneous maximized main bending angle, and minimized lateral bending angle

4. Conclusion

In this paper, the LTBP was investigated using response surface methodology and the effects of process parameters include laser power, scanning speed, laser beam diameter, irradiation length, number of irradiation passes, and the irradiation scheme on the main bending angle and lateral bending angle of the laser-bent tubes were investigated comprehensively. The main outcome of this study can be emphasized as follows:

1- The main bending angle increases by increasing the laser power, irradiation length, and the number of irradiation passes. Also, the AIS scheme creates a considerably higher main bending angle than the CIS scheme for similar conditions. The main bending angle decreases by increasing the scanning speed and laser beam diameter.

2- The main bending angle depends on the first and second-order of all selected process parameters and the interaction of process parameters except laser power and the number of irradiation passes can be neglected. The effect of the interaction of laser power and the number of irradiation passes is positive and increases the main bending angle due to increasing the transferred heat to the bent tube.

3- The lateral bending angle increases by increasing the laser power, irradiation length, and the number of irradiation passes. Also, the CIS scheme creates a considerably higher lateral bending angle than the AIS scheme. The lateral bending angle decreases by increasing the scanning speed and laser beam diameter.

4- The lateral bending angle is an unwanted, undesired, and complex effect in LTBP. Prediction of lateral bending angle is hard because of its dependence on six interactions of process parameters.

5- Higher main bending angle and lower lateral bending angle obtained by axial irradiation scheme (AIS). Increasing the number of irradiation passes, increases the main bending angle but it has more effect on the lateral bending angle than the main bending angle.

References

[1] M. Graser, N. Pflaum, M. Merklein, Influence of a local laser heat treatment on the bending properties of aluminium extrusion profiles, *Procedia CIRP*, **2018**, 74, 780–784, doi: 10.1016/j.procir.2018.08.011.

[2] S. Safdar, N. Li, M. A. Sheikh, Z. Liu, The effect of nonconventional laser beam geometries on stress distribution and distortions in laser bending of tubes, *J. Manuf. Sci. Eng. Trans. ASME*, **2007**, 129, 592–600, doi: 10.1115/1.2716715.

[3] S. Safdar, L. Li, M. A. Sheikh, Zhu Liu, Finite element simulation of laser tube bending: Effect of scanning schemes on bending angle, distortions and stress distribution, *Opt. Laser Technol.*, **2007**, 39, 1101–1110, doi: 10.1016/j.optlastec.2006.09.014.

[4] W. Li and Y. L. Yao, Numerical and experimental study of strain rate effects in laser forming, *J. Manuf. Sci. Eng. Trans. ASME*, **2000**, 122, 445–451, doi: 10.1115/1.1286731.

[5] W. Li and Y. L. Yao, Laser bending of tubes: Mechanism, analysis, and prediction, *J. Manuf. Sci. Eng. Trans. ASME*, **2001**, 123, 674–681, doi: 10.1115/1.1392992.

[6] Li, W., and Yao, Y. L., Convex laser forming with high certainty, *Proc. The North American Manuf. Research Conf. (NAMRC XXVIII)*, Lexington, Kentucky, May, **2000**, 33–38.

[7] J. Zhang, P. Cheng, W. Zhang, M. Graham, J. Jones, M. Jones, Y. L. Yao, Effects of scanning schemes on laser tube bending, *J. Manuf. Sci. Eng. Trans. ASME*, **2006**, 128, 20–33, doi: 10.1115/1.2113047.

[8] S. E. Khandandel, S. M. H. Seyedkashi, M. Moradi, A novel path strategy design for precise 2D and 3D laser tube forming process; experimental and numerical investigation, *Optik*, **2020**, 206, 164302, doi: 10.1016/j.ijleo.2020.164302.

[9] H. S. Hsieh, J. Lin, Study of the buckling mechanism in laser tube forming, *Opt. Laser Technol.*, **2005**, 37, 402–409, doi: 10.1016/j.optlastec.2004.06.004.

[10] R. Yadav, D. Kumar Goyal, R. Kant, A comprehensive study on the effect of line energy during laser bending of duplex stainless steel, *Opt. Laser Technol.*, **2022**, 151,108025, doi: 10.1016/j.optlastec.2022.108025.

[11] K. I. Imhan, B. T. H. T. Baharudin, A. Zakaria, M. I. S. B. Ismail, N. M. H. Alsabti, A. K. Ahmad, Investigation of material specifications changes during laser tube bending and its influence on the modification and optimization of analytical modeling, *Opt. Laser Technol.*, **2017**, 95, 151–156, doi: 10.1016/j.optlastec.2017.04.030.
[12] M. Keshtiara, S. Golabi, R. Tarkesh Esfahani, Multi-objective optimization of stainless steel 304 tube laser forming process using GA, *Eng. Comput.*, **2021**, 37, 155–171, doi: 10.1007/s00366-019-00814-0.
[13] S. E. Khandandel, S. M. H. Seyedkashi, M. Moradi, Numerical and experimental analysis of the effect of forced cooling on laser tube forming, *J. Braz. Soc. Mech. Sci. Eng.*, **2021**, 43, 338, doi: 10.1007/s40430-021-03063-9.
[14] A. Khorram, M. Ghoreishi, M. R. Soleymani Yazdi, M. Moradi, Optimization of bead geometry in CO2 laser welding of Ti6Al4V using response surface methodology, *Engineering*, **2011**, 3, 708–712, doi: 10.4236/eng.2011.37084.
[15] M. Moradi, M. Karami Moghadam, M. Shamsborhan, Z. Malekshahi Beiranvand, A. Rasouli, M. Vahdati, A. Bakhtiari, M. Bodaghi, Simulation, statistical modeling, and optimization of CO2 laser cutting process of polycarbonate sheets, *Optik*, **2021**, 225, 164932, doi: 10.1016/j.ijleo.2020.164932.
[16] M. Safari, A Study on Main and Lateral Bending Angles in Laser, *J. Stress Anal.*, **2021**, 5, 33–40.
[17] M. Safari, M. Farzin, A study on laser bending of tailor machined blanks with various irradiating schemes, *J. Mater. Process. Technol.*, **2014**, 214, 112–122, doi: 10.1016/j.jmatprotec.2013.08.007.
[18] M. Safari, R. A. de Sousa, J. Joudaki, Fabrication of saddle-shaped surfaces by a laser forming process: An experimental and statistical investigation, *Metals*, **2020**, 10, 1–13, doi: 10.3390/met10070883.
[19] M. Safari, R. A. de Sousa, J. Joudaki, Recent advances in the laser forming process: A review, *Metals*, **2020**, 10, 1–19, doi: 10.3390/met10111472.
[20] M. Safari, R. J. Alves de Sousa, J. Joudaki, Experimental investigation of the effects of irradiating schemes in laser tube bending process, *Metals*, **2021**, 11, 1123, doi: 10.3390/met11071123.
[21] M. Safari, A study on the laser tube bending process: effects of the irradiating length and the number of irradiating passes, *Iran. J. Mater. Form.*, **2020**, 7, 46–53, doi: 10.22099/ijmf.2019.34213.1133.
[22] I. Sakaev, A. A. Ishaaya, Diode laser assisted oxygen cutting of thick mild steel with off-axis beam delivery, *Opt. Laser Technol.*, **2021**, 138, 106876, doi: 10.1016/j.optlastec.2020.106876.

Appendix

Table A.1. The list of experiments was designed according to response surface methodology (Box-Behnken).

Experiment No.	Laser Power (P)	Scanning Speed (S)	Laser Beam Diameter (D)	Irradiation Length (L)	Number of Irradiation Passes (N)	Irradiation Scheme (Sch)
Unit	W	mm/s	mm	degree	-	-
1	800	15	6	20	1	AIS
2	800	15	6	100	3	CIS
3	1100	15	8	100	3	AIS
4	800	15	4	100	1	AIS
5	800	15	6	20	5	CIS
6	800	20	8	100	3	AIS
7	500	15	6	180	3	CIS
8	800	10	6	100	5	AIS
9	800	10	4	100	3	AIS
10	800	15	8	100	5	CIS
11	800	15	4	100	5	CIS
12	800	15	6	100	3	CIS
13	800	15	6	180	5	CIS
14	800	15	6	180	1	CIS
15	500	20	6	100	3	AIS
16	800	15	6	20	1	CIS

17	1100	15	6	20	3	CIS
18	800	15	8	180	3	CIS
19	800	10	6	20	3	CIS
20	800	15	4	100	5	AIS
21	800	10	6	100	5	CIS
22	500	15	6	100	1	AIS
23	800	15	6	100	3	AIS
24	1100	15	6	100	5	CIS
25	800	15	4	20	3	AIS
26	800	20	6	180	3	CIS
27	800	20	6	100	5	AIS
28	800	20	6	180	3	AIS
29	500	20	6	100	3	CIS
30	800	15	6	100	3	AIS
31	800	15	8	100	5	AIS
32	800	15	6	100	3	AIS
33	800	20	6	20	3	CIS
34	800	15	6	100	3	AIS
35	800	10	6	180	3	CIS
36	500	15	6	20	3	CIS
37	800	15	4	180	3	AIS
38	800	10	8	100	3	AIS
39	800	15	6	20	5	AIS
40	800	20	6	100	5	CIS
41	1100	10	6	100	3	CIS
42	1100	15	6	180	3	AIS
43	500	15	6	100	1	CIS
44	800	20	8	100	3	CIS
45	500	15	6	100	5	CIS
46	800	20	6	20	3	AIS
47	500	10	6	100	3	CIS
48	1100	15	4	100	3	AIS
49	1100	15	6	20	3	AIS
50	1100	20	6	100	3	CIS
51	1100	15	6	180	3	CIS
52	800	15	8	100	1	CIS
53	800	15	8	20	3	AIS
54	800	15	6	100	3	AIS
55	1100	15	6	100	5	AIS
56	800	15	6	100	3	CIS
57	800	10	6	100	1	AIS
58	800	15	8	180	3	AIS
59	800	15	6	100	3	AIS
60	800	20	6	100	1	CIS
61	500	15	8	100	3	AIS
62	500	10	6	100	3	AIS
63	500	15	4	100	3	CIS
64	800	15	4	180	3	CIS
65	800	15	6	100	3	CIS
66	1100	15	6	100	1	AIS
67	800	15	6	180	1	AIS

68	800	15	6	100	3	CIS
69	1100	15	4	100	3	CIS
70	500	15	4	100	3	AIS
71	800	15	4	100	1	CIS
72	800	10	6	100	1	CIS
73	800	20	6	100	1	AIS
74	800	15	6	100	3	CIS
75	1100	15	8	100	3	CIS
76	800	15	8	100	1	AIS
77	800	10	4	100	3	CIS
78	800	10	6	20	3	AIS
79	500	15	6	100	5	AIS
80	800	15	6	180	5	AIS
81	800	10	8	100	3	CIS
82	800	15	8	20	3	CIS
83	500	15	8	100	3	CIS
84	500	15	6	180	3	AIS
85	1100	10	6	100	3	AIS
86	800	20	4	100	3	AIS
87	800	20	4	100	3	CIS
88	800	15	4	20	3	CIS
89	1100	20	6	100	3	AIS
90	500	15	6	20	3	AIS
91	800	10	6	180	3	AIS
92	1100	15	6	100	1	CIS